A New Strategy for Weak Events in Sparse Networks: The First-Motion Polarity Solutions Constrained by Single-Station Waveform Inversion

by Lucia Fojtíková and Jiří Zahradník

INTRODUCTION

Moment tensor determinations of small earthquakes are quite challenging. It is because their signal-to-noise ratio is satisfactory only at frequencies above the microseismic noise peak (~0.2 Hz), and waveforms can be modeled only up to ~1–2 Hz at relatively near stations (epicentral distance of a few kilometers). Therefore, the availability of high-quality waveforms at near stations is the most critical issue. Dense local networks enable solving specific issues like non-double-couple (non-DC) components (e.g., Vavryčuk, 2011), relation with tectonics (Serpetsidaki *et al.*, 2013), and/or even space–time clustering of moment tensors (Cesca *et al.*, 2014). On the contrary, records of weak events at very few local stations hardly allow us to get even DC components of moment tensors.

For example, focal mechanism of two microearthquakes, M_w 0.2 and 0.4, were obtained by the full-waveform inversion in the frequency range below 4 Hz and distance below 3.7 km by Benetatos *et al.* (2013). Fojtíková *et al.* (2010) studied shallow earthquakes of M_w 1.2–3.4 at 0.8–1.6 Hz. A probabilistic nonlinear inversion of local waveforms was developed by Wéber (2009) and applied to weak events in Hungary. Various constraints for determining focal mechanisms of small local earthquakes monitored by sparse networks were adopted. For example, Nakamura (2002) suggested a joint use of the *P*- and *S*-wave polarities. Li *et al.* (2011) combined the phase and amplitude waveform matching with the first-motion *P* polarities and average *S*/*P* amplitude ratios. Delouis and Legrand (1999) emphasized inclusion of the near-field Green's function terms. Pinar *et al.* (2003) made tests according to which some single-station inversions are feasible. Busfar and Toksoz (2013) gave examples of focal mechanisms calculated in good velocity models from less than four stations. Godano *et al.* (2010, 2011) studied the minimum number of needed sensors and addressed reliability of full moment tensors by the uncertainty analysis. Zahradník and Custódio (2012) presented examples of both successful and nonsuccessful single-station inversions and provided an explanation with resolvability analysis (6D error ellipsoids). Their successful and nonsuccessful examples differed by the frequency range of the inversion. The latter work also provided references to pioneering papers about single-station inversion dating back to 90s.

This brief state-of-art overview clearly shows that methodology of the focal mechanism determination of the weak events in sparse networks belongs to currently challenging tasks. The objective of this paper is to propose a simple technique, basically opposite to those most commonly used, that is, to start with a broad suite of the first-motion polarity solutions of an earthquake and constrain the solution by a single-station waveform inversion. The method will not only reduce the uncertainty of the polarity-based mechanism but will also provide the moment magnitude.

Our interest in weak events has strengthened in recent years in relation to earthquakes of the local magnitude $M_L \sim 1$–3 recorded near the Slovakia–Hungary border. The area is situated close to epicenter of the historical damaging earthquake of Komárno (28 June 1763; macroseismic intensity up to VIII–IX, MSK-64; Brouček *et al.*, 1991). Focal mechanisms are needed for ground-motion simulations of similar future events as well as for seismotectonic analyses. The focal mechanisms have not been determined in this particular region yet. Therefore, we study feasibility of the focal mechanism determination by the newly proposed method.

This paper is structured as follows. First, we describe the innovative method to constrain the first-motion polarity solutions by single-station waveforms. Then, the method is validated on an example of an M_w 4.3 earthquake in Corinth Gulf, Greece, for which the focal mechanism was previously calculated by standard waveform inversion (i.e., without prior polarity constraint) from 10 stations. Finally, the method is applied to the weak ($M_w \sim 3$) event in Slovakia. In this case, many polarities were available, but only one three-component waveform could be well modeled. Subsequently, some difficulties and limits of the method are discussed.

CYCLIC SCANNING OF THE POLARITY SOLUTIONS

Here, we introduce a simple innovative approach designed for better resolving focal mechanisms of weak events called cyclic

doi: 10.1785/0220140072

scanning of the polarity solutions (CSPS). The principle of CSPS is as follows: the FOCal MEChanism (FOCMEC) code (Snoke, 2003) provides a suite of the DC solutions satisfactorily explaining the observed first-motion polarities. The variability of the focal mechanism within the suite could be large due to allowing some polarity misfits in practice. For decreasing the uncertainty, that is, to reduce the scatter of the nodal lines, the waveform constraint is applied. For this goal, the FOCMEC solutions (the strike/dip/rake angle triplets) are taken, one by one, and used as input for the waveform inversion.

Having prescribed the strike, dip, and rake, the waveform inversion is made for the scalar moment, source position, and centroid time. ISOLated Asperities (ISOLA) software is chosen for these tasks (Sokos and Zahradník, 2008, 2013). The moment is calculated by the least squares, whereas the position and time is grid searched. The low-frequency limit of the inversion range is determined by the noise (either natural or instrumental). The high-frequency limit is determined by a given epicentral distance and quality of the velocity model. The same frequency range of real data and synthetics is considered, detailed in the following applications. Full-waveform Green's functions are calculated by the discrete wavenumber method. The inversion is performed with the (band passed) displacements aligned to origin time. For methodical details, see, for example, Křížová *et al.* (2013), Zahradník and Sokos (2014), and the references therein covering the whole period of the ISOLA development and numerous applications since 2003.

Each member of the FOCMEC solution suite is quantified by the waveform fit (variance reduction [VR]), and a subset of admissible solutions is calculated. Because the focal mechanisms are already *a priori* constrained by polarities, the uncertainty of the admissible solutions can be often significantly reduced compared to FOCMEC, even with a single three-component station. This is the main advantage of CSPS method.

To define the admissible CSPS solutions, we choose an interval close to the optimum solution, for example, the interval between 0.95 VRopt and VRopt, in which VRopt refers to the variance reduction of the best-fitting solution. The choice of the threshold (0.95) is obviously subjective, but it is well usable if comparing several solutions with each other in a relative sense, keeping the threshold value constant. The setup of the threshold is equivalent to weighting the waveform fit with respect to polarity fit (a very small threshold means that the solution is practically determined by the polarities only). For a more sophisticated setup of admissible solutions, based on a statistical assessment of errors, we would need a very problematic specification of the waveform data variance (Zahradník and Custódio, 2012).

VALIDATION EVENT IN THE CORINTH GULF, GREECE

The CSPS method has been tested on the event the mechanism of which was studied using 10 stations (Sokos and Zahradník, 2013). It was a shallow M_w 4.3 event that occurred on 25 April 2012 at 10:34 UTC at latitude 38.4045° N, longitude 21.9877° E (see Fig. 1a for the source–station configuration). The ten-station mechanism, taken as a reference for the present paper, is described in Table 1. The earthquake is a normal-faulting event, typical for the extensional regime of the Corinth Rift (Sokos *et al.*, 2012). The FOCMEC solution with one admissible polarity misfit features a very large uncertainty (see Fig. 2a). The three-component waveforms were available at six stations (DSF, GUR, KALE, LAKA, SERG, and TRIZ), whereas four others have had some problematic component. These six stations have been repeatedly used in the CSPS method. Each single-station three-component waveform has been inverted in the same frequency range as in case 2 of Sokos and Zahradník (2013): 0.04–0.16 Hz. The frequencies below 0.04 Hz were too noisy, and frequencies above 0.16 could not be modeled with existing crustal model. The velocity model has been the one routinely used in the studied region (Novotný *et al.*, 2001). All (99) fixed focal mechanisms of the FOCMEC solution have been inspected in a loop, using ISOLA in the mode with the prescribed strike/dip/rake angles. The only parameter to be inverted by the least-squares method has been the scalar moment, whereas the source depth and time has been grid searched. The grid search has been made in a vertical line of trial source positions situated below the epicenter (depth 1–20 km, step of 1 km) and in an interval of ±3 s around origin time with the 0.15 s step. The admissible solutions in the interval between 0.95 VRopt and VRopt for each single-station application of the CSPS method are shown in Figure 1b. There are 7–23 solutions for each case. The optimal (VRopt) solutions from the six CSPS applications are compared in Figure 2b and summarized in Table 1. Only five pairs of nodal lines are seen in Figure 2b because two of the solutions have the same strike/dip/rake angles (see the CSPS solutions using SERG and KALE stations in Table 1). The departure from the reference solution, shaded in Figure 2b, is quantified by Kagan angle (Kagan, 1991), also given in Table 1, varying between 8° and 32°. The results demonstrate that our inverse problem has enough sensitivity with respect to the strike, dip, and rake angles, and the CSPS approach considerably reduces the uncertainty compared to the FOCMEC method. The solutions represent a reasonable proxy of the right focal mechanism (i.e., the ten-station, reference mechanism). The moment magnitude is stable among the tests (M_w 4.3–4.6), but the grid-searched focal depth is much less stable (5–20 km).

It is important to underline that CSPS is not the same as the standard single-station inversion. If each single station is inverted for the focal mechanism, that is, without any polarity constraint, the problem is generally ill posed. It is well illustrated by the condition number that varies between 5 and 30, attaining the largest values at the nearest stations SERG and TRIZ. Therefore, the standard single-station waveform inversions considerably differ of each other. This is demonstrated (for the ISOLA DC-constrained moment tensor inversion) in Figure 2c and in Table 1. The Kagan angle in the latter situation is as large as 16°–61°. The standard single-station inversions were used as demonstration that although occasionally they could be close enough to the right solution they do not offer

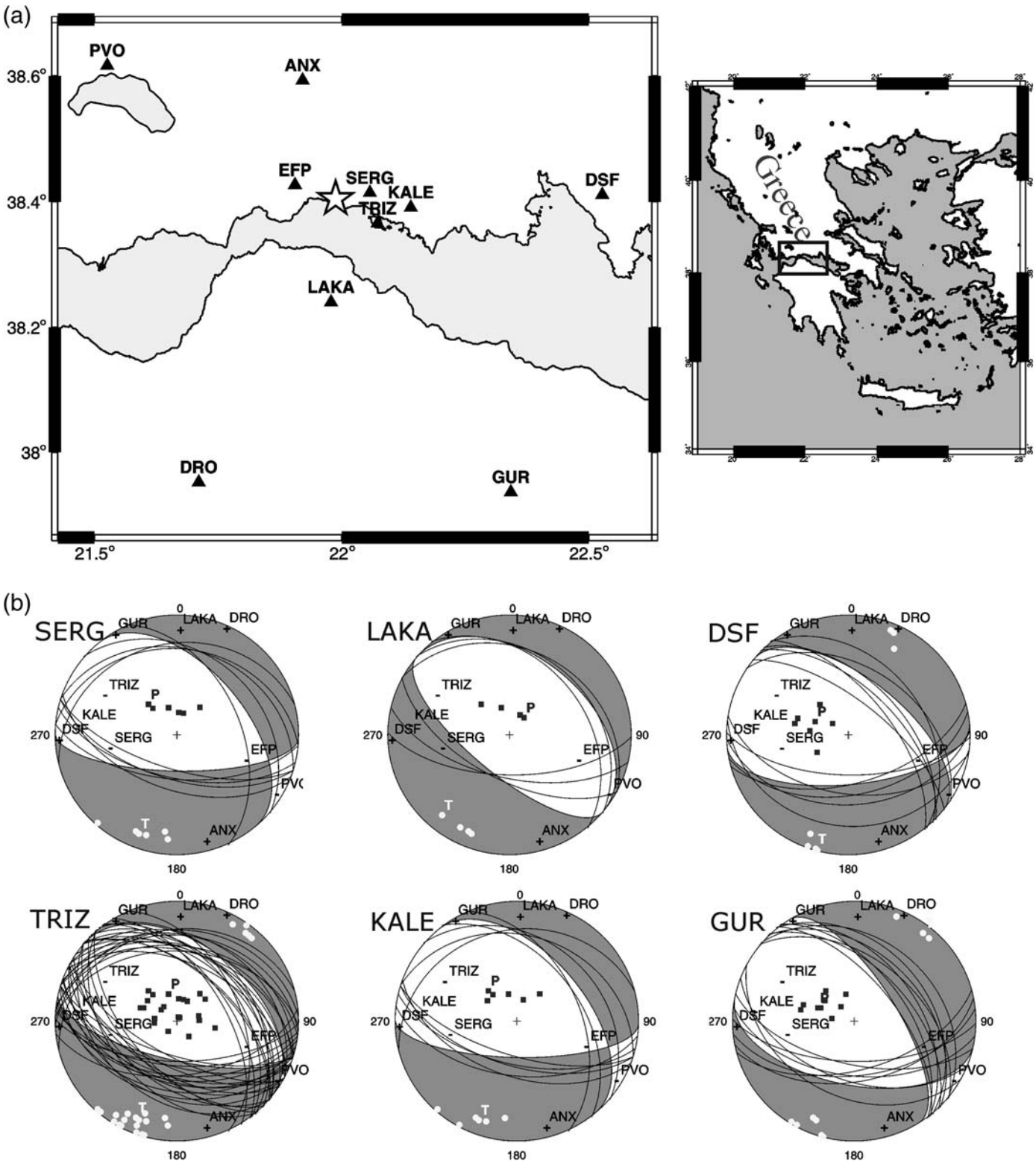

▲ **Figure 1.** Test event in Corinth Gulf, Greece—stations and new method. (a) Used stations are marked by triangles, epicenter by star (modified from Sokos and Zahradník, 2013). The inset shows a larger map. (b) The new approach of this paper, the cyclic scanning of the polarity solutions (CSPS) method, applied to six individual stations. Nodal lines are plotted for admissible CSPS solutions the variance reduction of which is between 0.95 VRopt and VRopt. Compressional sectors of the best-fitting solution (VRopt) are shaded.

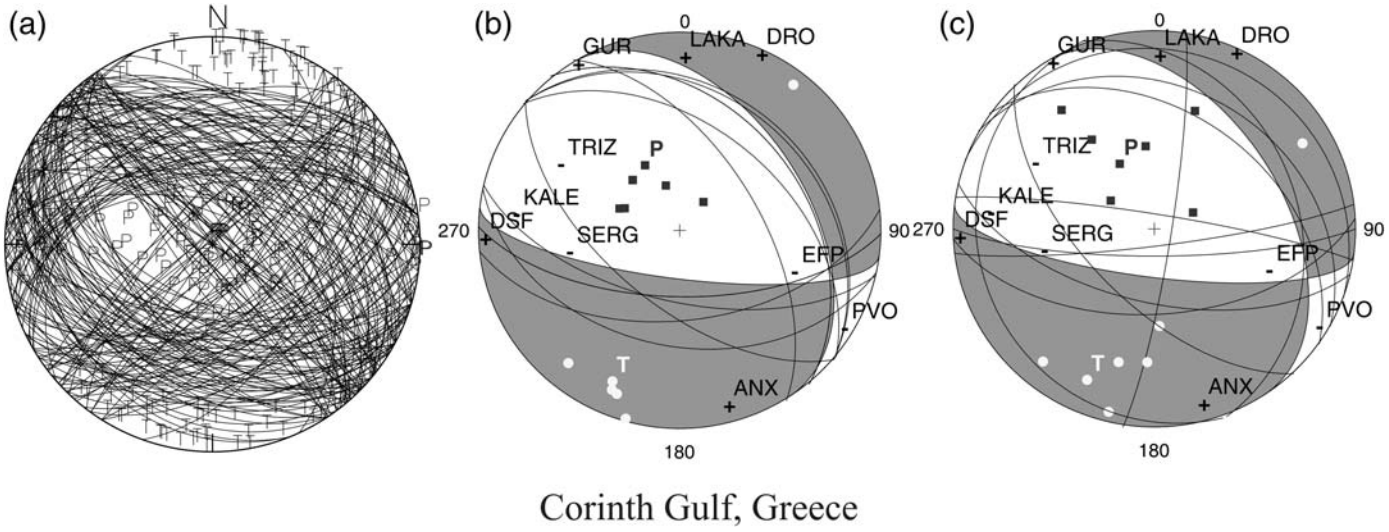

▲ **Figure 2.** Test event in Corinth Gulf, Greece—comparison of three methods. (a) First-motion polarity solutions with one misfit allowed. Uncertainty of the focal mechanism is very large. (b) Best-fitting CSPS solutions from six individual stations shown by nodal lines, considerably reducing the uncertainty. The CSPS focal mechanisms are close to the reference solution derived by ten-station waveform inversion (shaded in the present figure). For numeric results, see Table 1. This is a recommended approach. (c) Example of a non-recommended approach, less suitable than CSPS: focal mechanisms from six standard single-station waveform inversions are demonstrated, some of them strongly deviating from the reference (shaded) solution.

a safe tool for small events in a sparse network. On the other hand, the results above provided enough encouragement for application of the CSPS approach.

WEAK EVENT IN SLOVAKIA

On 17 January 2013 at 10:50 UTC, a shallow crustal earthquake of the local magnitude M_L 2.8 (Geophysical Institute, Slovak Academy of Sciences) occurred near Kolárovo town in southern Slovakia (Fig. 3). It was preliminary located at latitude 47.902° N, longitude 18.021° E, depth 1 km. The studied event is the largest one in a group comprising a number of about 25 shocks of $M_L < 2$, which were recorded nearby in 2011–2012. Considerably stronger events occurred nearby in the past (e.g., Komárno, 28 June 1763, VIII–IX, MSK-64). Focal mechanisms have not been calculated for this region yet,

Table 1
Comparison of Three Centroid Moment Tensor Solutions for the Validation Event, Corinth Gulf, Greece

	Stations	Depth (km)	Time (s)	$M_0 \times 10^{16}$ (N·m)	M_w	Strike (°)	Dip (°)	Rake (°)	Variance Reduction	Kagan Angle (°)
Reference solution	10 stations	8	0.60	0.42	4.3	327	32	−45	0.69	–
CSPS solutions *	DSF	7	2.55	0.46	4.4	309	47	−56	0.94	19
	GUR	17	0.30	0.67	4.5	328	58	−61	0.94	31
	KALE	5	1.20	0.29	4.3	320	38	−48	0.95	8
	LAKA	8	0.90	0.49	4.4	310	30	−90	0.97	32
	SERG	20	0.90	0.85	4.6	320	38	−48	0.91	8
	TRIZ	8	0.15	0.48	4.4	310	32	−67	0.98	12
Direct single-station	DSF	7	2.40	0.53	4.4	305	41	−60	0.94	16
inversion solutions	GUR	4	1.95	0.84	4.6	160	13	150	0.98	45
	KALE	7	1.35	0.36	4.3	339	29	−15	0.99	21
	LAKA	9	0.75	0.55	4.5	299	30	−105	0.98	39
	SERG	10	1.20	0.76	4.6	9	83	−31	0.97	61
	TRIZ	8	0.30	0.52	4.4	290	12	−70	0.98	25

*CSPS, cyclic scanning of the polarity solutions.

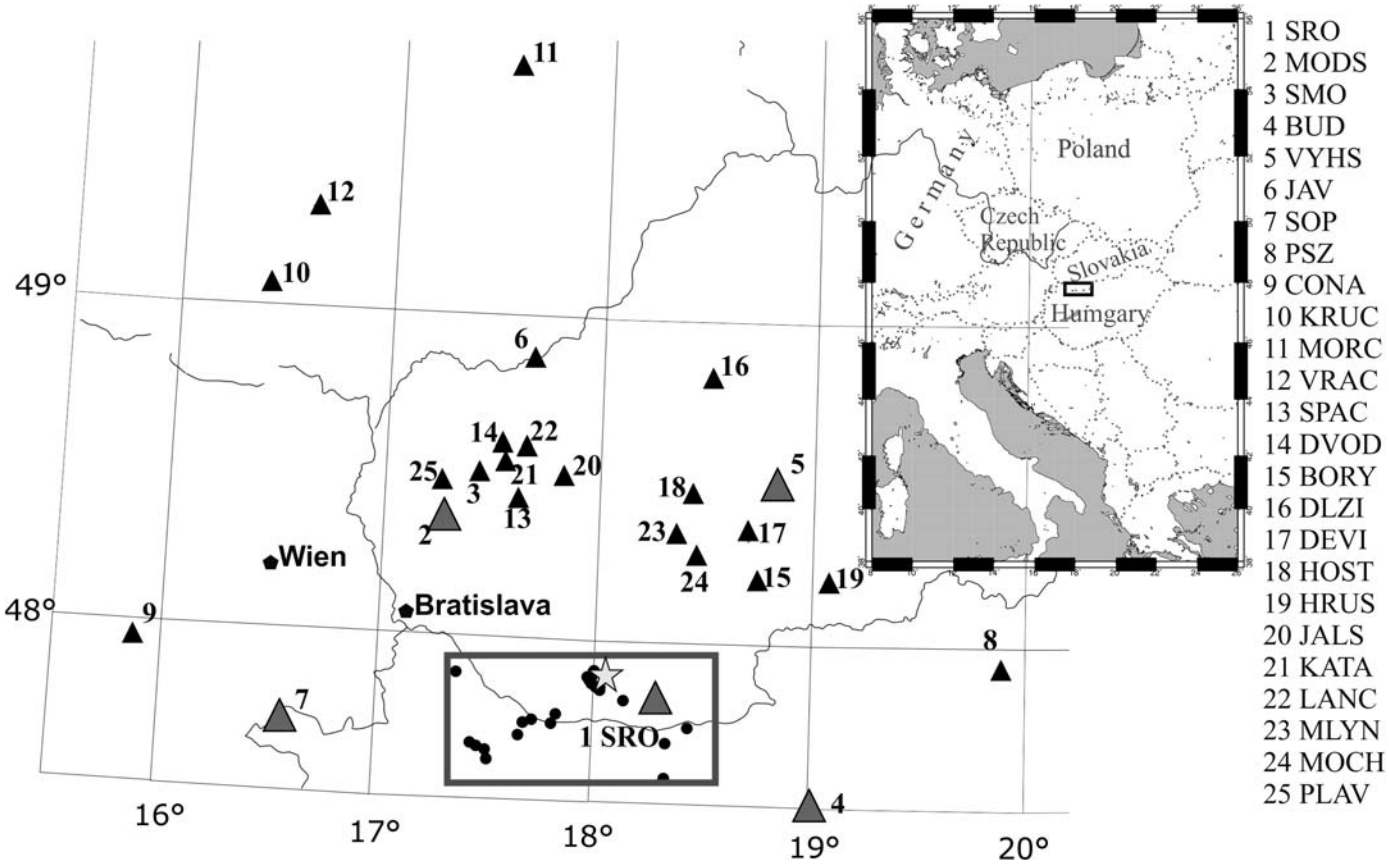

▲ **Figure 3.** Weak event in Slovakia—source–stations configuration. The study region (rectangle) is situated close to the Slovak–Hungarian border. Epicenter of the studied event is marked by star. Stations from which only first-motion polarities were used are shown by small black triangles, stations considered for the waveform inversion by larger dark gray triangles. The most important is the nearest station Šrobárová (denoted 1 SRO) at which the observed waveform can be successfully modeled. Circles demonstrate nearby recent events 2011–2012 M_L <2. Inset shows the broader region.

except four events in Hungary, not far from the studied region (Hungarian Earthquake Bulletin). Therefore, it is necessary to investigate in detail as many events in this region as possible, even if the data are not completely appropriate. In particular, the first-motion polarities from many stations are available, but only one station could be used to fairly well match the observed and synthetic waveforms.

The studied event was relocated using five near stations with the clear and consistent arrival times (SRO, MODS, BUD, VYHS, SOP, epicentral distance ~20–110 km). The following six-step approach was applied. (i) The *P*-wave arrival times were repicked. (ii) Velocity model H^* (Novotný and Urban, 1988) was adopted as a working *P*-velocity model related to the studied region. Two other *P*-velocity models, taken from Greece and Italy, hence not related to the studied region at all, were used just to check stability of the *P*-wave location of the epicenter (Novotný *et al.*, 2001; Vuan *et al.*, 2011). Despite significant differences among the models, a very stable epicenter position has been obtained, near the preliminarily estimated position. (iii) Using model H^* and the initial part of waveforms (the *P*-wave group), the epicenter has been also calculated by the source scanning algorithm with the several fixed depths. This method (Janský *et al.*, 2012), fully based on waveforms, and working without any arrival time reading, confirmed proximity of the epicenter to its initial position as well as usability of the H^* velocity model. (iv) The *S*-wave arrival times were repicked, but the uncertainty was high due to the strong *P*-wave coda waves. The *S* wavepick at the nearest station (SRO) was also validated by means of the particle-motion diagram. (v) The *P*- and *S*-wave readings were used to construct the Wadati diagram. Inconsistent *S*-wave readings were detected and a new *S*-wave repicking was made to reduce the scatter of the diagram. The V_P/V_S ratio was estimated as 1.67. (vi) The *S*-velocity model was constructed from the *P*-velocity H^* model, using the $V_P/V_S = 1.67$ value from the Wadati diagram. Then, the *P*- and *S*-wave arrival data were used to newly locate the event, allowing several starting depths. This procedure resulted in the relocation near the preliminary epicenter, but considerably deeper; 10:50:39.23 UTC, latitude 47.9062° N, longitude 18.0518° E, depth 15 km (root mean square 0.08 s, horizontal error (ERH) 0.4 km, vertical error (ERZ) 0.5 km).

Twenty-five first-motion polarities were analyzed (Fig. 4a). A polarity reversal at the nearest station (SRO) was detected by comparing clear three-component *P*-wave arrivals of a teleseis-

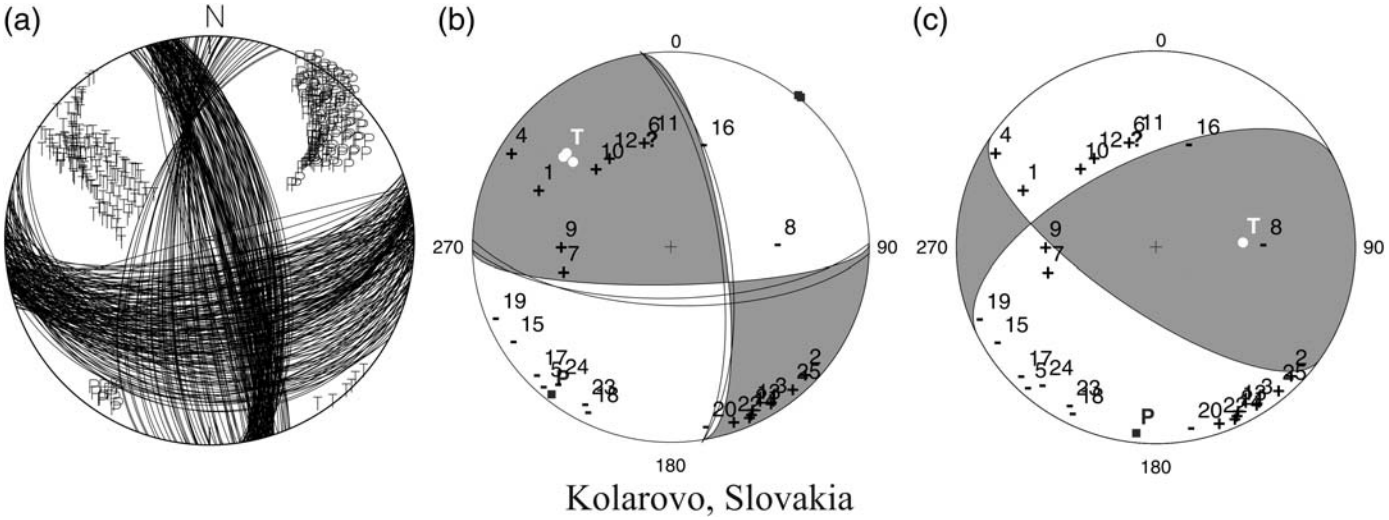

▲ **Figure 4.** Weak event in Slovakia—comparison of three methods. (a) First-motion polarity solutions with one misfit allowed. Uncertainty of the focal mechanism is large. (b) The recommended approach of this paper, the CSPS method, applied with the nearest station (SRO). The uncertainty of the polarity solution is considerably reduced by modeling the SRO waveform. Nodal lines are plotted for admissible CSPS solutions the variance reduction of which is between 0.95 VRopt and VRopt. Compressional sectors of the best-fitting focal mechanism (VRopt) are shaded. (c) A nonrecommended approach, that is, standard waveform inversion of a single station (SRO), providing a solution that disagrees with many observed polarities. For station numbers and codes see legend of Figure 3.

mic event at four neighboring stations; then the SRO record was flipped. The polarities were used to calculate the focal mechanism solution by FOCMEC code, allowing one polarity misfit. The velocity model H^* and the relocated hypocenter depth of 15 km were applied. The polarity solution in Figure 4a indicates the likely focal mechanisms, much better than in the Corinth Gulf validation, but the uncertainty is still large. It obviously needs a further constraint. We show that waveform at the nearest station SRO may help.

Initially, seismograms at five nearest stations (SRO, MODS, VYHS, BUD, and SOP) were considered for possible use. However, due to small magnitude, no signal was detected in the frequency range below the microseismic noise peak hence the usable frequency range starts above 0.3 Hz. Station MODS had to be removed due to noise at all. The requirement to match the observed waveforms by synthetics implied (after some experimentation) the upper frequency limit of 0.55 Hz. In this range, the nearest station SRO record can be matched by synthetics with a reasonable correlation, but the other stations remain uncorrelated. Therefore, we use only station SRO. The instrument response was removed, and the band-passed (0.3–0.55 Hz) record was integrated to displacement and inverted in this frequency range.

To constrain the polarity solutions, the CSPS method was applied with the nearest station SRO, again using velocity model H^*. The depth grid search was the same as in the validation tests (1–20 km beneath epicenter, with the 1 km increment). When considering ~100 FOCMEC solutions, they featured more clustering than in the Corinth example. Therefore, to be sure that we cover the whole variability of possible mechanisms, we increased their number by choosing smaller increments of the source angles, but the clustering of nodal lines remained almost unchanged. From 169 solutions of FOCMEC only 3 almost identical solutions remained in the interval between 0.95 VRopt and VRopt, in which VRopt = 0.53 (Fig. 4b). This is a very efficient reduction of the uncertainty compared to the FOCMEC suite of nodal lines. Moreover, the three solutions satisfy all polarities. The optimum solution has the following parameters: source depth 10 km, time 0.35 before the location origin time, strike/dip/rake = 351°/66°/161°, scalar moment 0.74×10^{14} N·m, moment magnitude 3.2. The source depth and time have a certain trade-off (Fig. 5a). The latter partly explains the 5 km departure from the 15 km hypocenter depth. (The other factor controlling the centroid depth is the frequency range; with increasing frequency we obtained larger depths, 15–20 km, but the waveform match was less good.) The optimum waveform match is demonstrated in Figure 5b. The VR 0.53 is lower than in the validation tests from the Corinth Gulf. It is because the present event has a smaller magnitude, a lower signal-to-noise ratio, and the station is situated at a larger distance with respect to wavelength (for more details see the Discussion section).

As in the validation test, we also prove that CSPS is considerably better than the standard single-station waveform inversion. The source–station (SRO) configuration and the frequency range are characterized by condition number as large as 14, so it is not surprising that the standard inversion without any polarity constraint is ill posed and provides a wrong focal mechanism, strike/dip/rake = 125°/61°/132°, which disagrees with many observed polarities (Fig. 4c). Its deviation from the correct solution strike/dip/rake = 351°/66°/161° (Fig. 4b) in sense of the Kagan angle is as large as 92°.

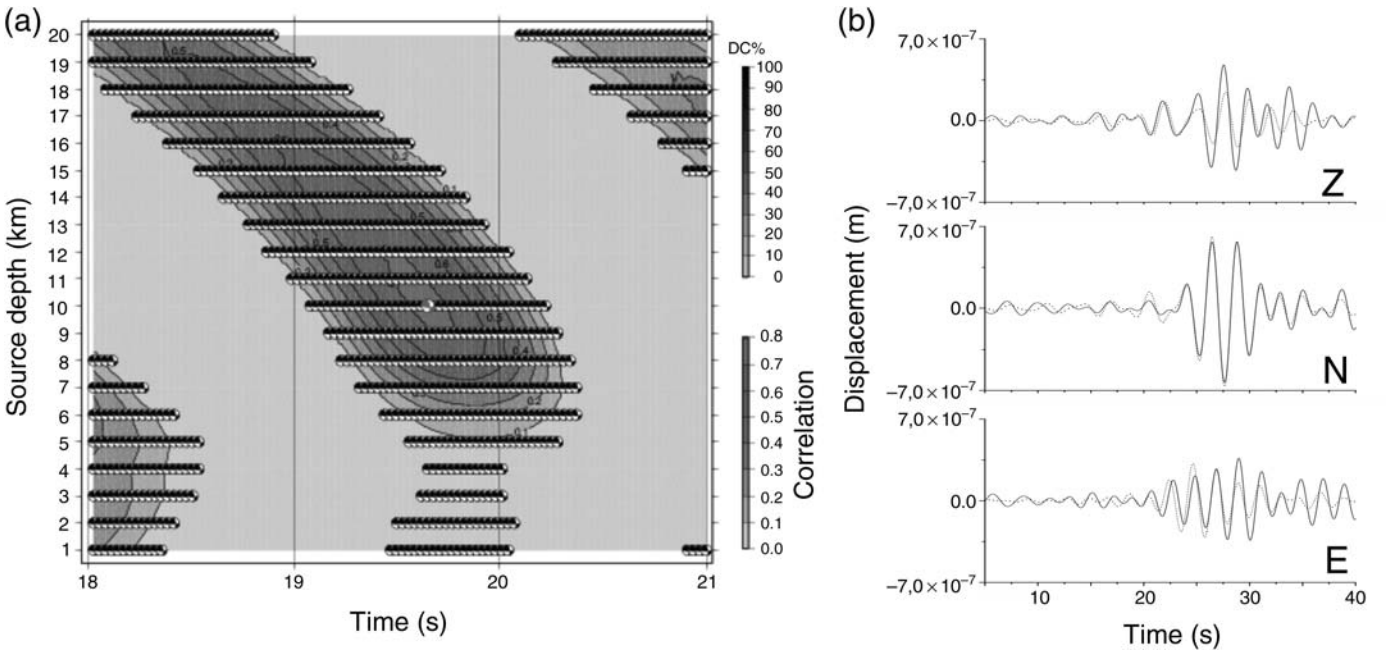

▲ **Figure 5.** Weak event in Slovakia—fitting waveform data. (a) The depth–time correlation diagram for the best-fitting CSPS focal mechanism obtained with the single station SRO (strike/dip/rake = 351°/66°/161°, moment magnitude 3.2.), that is, the solution shaded in Figure 4b. (b) Waveform matches at the nearest station (SRO) for the best-fitting CSPS solution in the frequency 0.3–0.55 Hz range. The origin time is formally denoted as 20 s.

DISCUSSION

The number of solutions provided by FOCMEC is (technically) determined by the size of increments of the tested mechanisms and (physically) determined by the number of allowed polarity misfits. As regards the technical condition, ~50–100 solutions usually represent the variability of the solutions well. Increasing their amount would only slow down the CSPS processing. The allowed polarity misfits are more important. Allowing fewer polarity misfits, in limiting case not permitting any disagreement between the observed and calculated polarities, the family of the FOCMEC solutions is less abundant. The polarity solution is (formally) strongly constrained, but it may be wrong if some polarities are wrong, so also the CSPS solution may be wrong. A good example in context of the Slovakia event is the unclear polarity at station 11 (MORC). When allowing one polarity misfit, the best-fitting CSPS solution (strike/dip/rake = 351°/66°/161°) disagrees with MORC negative polarity. If, however, allowing no polarity misfit, MORC '–' is fitted, we have only 10 FOCMEC solutions, not including the best solution (351°/66°/161°), and the waveform fit at SRO with the CSPS solution is slightly worse.

The success of the CSPS method naturally depends on the reliability of the FOCMEC solutions themselves. Let us assume a limiting case of polarities very unfavorably distributed on the focal sphere (e.g., most of them in a single P or T sector). Such polarities provide a very poor constraint on the focal mechanism. Then, the solution best fitting the waveform may be wrong, even if the VR is very high, VR ~ 1 (in case of the unconstrained ill-posed waveform inversion).

The case of wrong (reversed) polarities is unpleasant. Some of the polarity mistakes can be easily identified because no focal mechanism can be found. However, with some wrong polarities a focal mechanism can be determined, but it can be wrong, so also the CSPC result. The waveform constraint could eliminate the erroneous solutions from FOCMEC but not necessarily always.

As regards the waveform inversion, we can ask: "What is the minimum value of VRopt for considering the waveform inversion still reliable?" We have no simple answer to this question. It might seem that in inverting a single station it is easy to obtain VRopt close to 1, but that is not always the case, even when the focal mechanism is tightly constrained already by polarities. A single-station waveform might not be fitted well, unless using specifically calibrated velocity models (Dias *et al.*, submitted). A practical rule of thumb is that we can fit the stations reasonably well up to the distance of a few minimum shear wavelengths (MSWs) only. Recall the Corinth example of this paper with distances up to ~60 km, equivalent to ~3 MSWs; hence the single-station fits were as high as VR ~ 0.9 (Table 1). On the other hand, in the Slovakia example, we worked at ~20 km, equivalent to ~5 MSWs, and we got a lower fit.

More applications of the CSPS method, besides the present paper, can be mentioned: Fojtíková (2014) studied an M_L 3.3 event with two stations up to 44 km, using 0.4–0.9 Hz; she could reach VRopt = 0.3. The CSPC method allowed her

to estimate M_w 2.7–3.0. J. M. Carvalho and L. V. Barros (2014, a paper under preparation) used the CSPS method for obtaining the focal mechanism of an m_b 5.0 very shallow earthquake in Mara Rosa, Goiás State, Brazil, in 2010, followed by an aftershock sequence. Although the aftershocks were recorded with a local temporary network, allowing excellent applicability of standard ISOLA software (Carvalho *et al.*, 2014), the mainshock was recorded with the nearest stations situated as far as 120 and 140 km. This has been calling for the application of the CSPS method. Using good signal at 0.05–0.18 Hz and fitting the waveforms at 120 and 140 km with VRopt ~ 0.3, the CSPS method considerably reduced the FOCMEC uncertainty and provided an important estimate of M_w (~4). Moreover, the CSPS solution was found well compatible (Kagan angle ~30°) with the composite focal mechanism of the sequence (Barros *et al.*, 2014). Dias and Assumpção (2014) and Dias *et al.* (submitted) studied an m_b 4.8 event in Pantanal Basin, Brazil, for which the closest available broadband station was situated as far as ~800 km. They used a single-station waveform inversion with an *ad hoc* velocity model inverted from the surface-wave dispersion, hence reached VR = 0.9. To further strengthen the result and precise the nodal planes, they implemented polarities by means of the CSPS method. Villegas *et al.* (2014) studied an M_w 3.6 event the FOCMEC solution of which based on the only eight available polarities was determined with a significant uncertainty. Their solution was then well constrained by using the CSPS method, employing waveform modeling (0.05–0.08 Hz) at 5 stations (70–200 km).

CONCLUSION

A focal mechanisms determination of small events observed in sparse networks is difficult. To improve the situation, we developed and tested a new method in which the first-motion polarity solutions are constrained by repeated single-station waveform inversions with the prescribed DC mechanism. This simple approach is called CSPS. A relatively large suite of the first-motion polarity solutions from FOCMEC represents the input data. The strike/dip/rake angles of the individual solutions are kept fixed while inverting waveforms for the scalar moment, source depth, and time. The method was validated on a previously studied event in the Corinth Gulf, for which a well-determined focal mechanism was available. Then, the method was applied to a weak event of interest in southern Slovakia. The latter was recorded just in a single near station allowing the waveform modeling. It has been demonstrated that the CSPS method considerably reduces the uncertainty of the polarity solution.

We also emphasized that the CSPS method strongly differs from the standard single-station waveform inversions (in which the strike/dip/rake angles belong to the inverted parameters and a prior polarity constraint is missing). The standard single-station waveform inversion might occasionally produce correct mechanisms, but sometimes not; as a generally ill-posed approach, it cannot be recommended as a safe tool. On the contrary, the presented CSPS method has a great application potential in sparse networks where weak events are recorded at many stations, thus providing polarities, but only few of the stations are situated near epicenter to allow full waveform modeling. We focused on a limiting case of a single near station, but, obviously, more near stations would further help.

We showed that the CSPS method provides a good proxy of the focal mechanism and scalar seismic moment (and the moment magnitude). The moment determination is a significant add-on feature with respect to the polarity solutions. However, as seen in the validation tests, the source position and time are less trustable. The formally optimal depth and time from the CSPS method can hardly be preferred against those from a precise location. That is why in case of well-located events the grid search can be limited to a relatively narrow range above and below the hypocenter. If the location is highly uncertain (e.g., allowing source depths 0–10 km) and FOCMEC solutions significantly change within this range, it is possible to select a few characteristic depths, to produce the FOCMEC solutions, and, correspondingly, to run the CSPS method repeatedly.

Logically, when using a single station (or very few stations), users of the CSPS method must be aware of the good quality of the input data, such as the epicenter location, sensor orientation, instrumental parameters (poles and zeros, gain). A typical risk at near stations is that records from any kind of instrument (broadband or short period), from any manufacturer, might be damaged by instrumental disturbances (Zahradník and Plešinger, 2010). As a rule, the disturbances are overlooked during routine waveform inversions, because they are not simply visible in the band-passed records. Disturbed record in the CSPS method might considerably bias the result. A safe way to detect the disturbances is to inspect the integrated instrument output, the so-called raw displacement, prior to removing the instrument response and prior to any filtration. Some disturbed records might be corrected (Zahradník and Plešinger, 2005), but the operation is delicate. The safest approach is to eliminate the disturbed records.

The outlook related to the seismically active region in southern Slovakia, close to epicenter of the historic damaging earthquake, is optimistic. As proved by this feasibility study, combined information from the first-motion polarities and a few waveforms might be used to resolve focal mechanisms of the small events ($M_w \sim 3$), although, obviously, future improvement of the station coverage in this important focal zone would be even more helpful.

A more general outlook is as follows: we believe that the CSPS method can improve determination of focal mechanisms of small events M_w 2–3. The waveforms will be inverted at ~0.4–1 Hz if having 1–3 stations with sufficiently small hypocentral distances. By sufficiently small distance, we mean ~3–5 MSWs, that is, ~10–20 km. Similarly, M_w 1–2 could be studied by the CSPS method in small local networks (< 10 km). Of course, enough polarities at more distant stations must be available.

ACKNOWLEDGMENTS

The first and second authors were partially financially supported from two different grants of the Czech Science Foundation: GACR-P210/12/2336 and GACR-14-04372S, respectively. Waveform data provided by the Hellenic Unified Seismic Network (HUSN) and Corinth Rift Laboratory Network (station TRIZ), used previously by Sokos and Zahradník (2013), are greatly appreciated. Seismic stations jointly operated by the Charles University in Prague and the University of Patras belong to HUSN. Waveform data provided by Geophysical institute of the Slovak Academy of Sciences and Seismological Observatory of the Hungarian Academy of Sciences were appreciatively used. The authors thank J. Janský and O. Novotný who relocated the Kolárovo earthquake and K. Csicsay who helped with instrumental parameters. J. M. Carvalho, F. Dias, and R. Villegas kindly provided their unpublished results. We also thank the editors and anonymous reviewers whose comments helped us to improve the presentation of the results. Special thanks go to E. Sokos for his continuing cooperation including the planned implementation of the cyclic scanning of the polarity solutions method into a next version of ISOLA-GUI.

REFERENCES

Barros, L. V., M. Assumpção, C. Chimpliganond, J. M. Carvalho, M. G. Von Huelsen, D. F. Caixeta, G. S. França, D. F. Albuquerque, V. M. Ferreira, and D. P. Fontenele (2014). The Mara Rosa 2010 GT-5 earthquake and its possible relationship with the continental-scale TransBrasiliano lineament, *J. S. Am. Earth Sci.* (submitted).

Benetatos, C., J. Málek, and F. Verga (2013). Moment tensor inversion for two micro-earthquakes occurring inside the Háje gas storage facilities, Czech Republic, *J. Seismol.* **17,** 557–577, doi: 10.1007/s10950-012-9337-0.

Brouček, I., U. Eisinger, V. Farkas, R. Gutdeutsch, C. Hammerl, and G. Szeidovitz (1991). Reconstruction of building damages caused by 1763 earthquake in Komárno/Danube from contemporary depictions of the same site and from respective texts, in *Proc. of the ESC XXII General Assembly*, Barcelona, 17–22 September, 353–360.

Busfar, H., and M. N. Toksoz (2013). Determining the mechanisms and depths of relatively small earthquakes using a few stations by full-waveform modelling, *Geophys. Prospect.* **61,** 712–724, doi: 10.1111/1365-2478.12018.

Carvalho, J., L. V. Barros, and J. Zahradník (2014). Seismic source parameters of local micro-earthquakes in Goiás State Brazil by waveform inversion (abstract), special issue, *Earth Sci. Res. J.* **18,** 166–167.

Cesca, S., A. T. Sen, and T. Dahm (2014). Seismicity monitoring by cluster analysis of moment tensors, *Geophys. J. Int.* **196,** 1813–1826, doi: 10.1093/gji/ggt492.

Delouis, B., and D. Legrand (1999). Focal mechanism determination and identification of the fault plane of earthquakes using only one or two near-source seismic recordings, *Bull. Seismol. Soc. Am.* **89,** 1558–1574.

Dias, F. L., and M. Assumpção (2014). Moment tensor solution of moderate events at large distances: Using surface waves dispersion to build velocity models for the waveform inversion, examples from (abstract), special issue, *Earth Sci. Res. J.* 18**,** 162–163.

Dias, F., M. Assumpção, E. M. Facincani, G. S. França, M. L. Assine, A. C. P. Filho, and R. M. Gamarra. The 2009 earthquake, magnitude 4.8 m_b, in the Pantanal Wetlands, west-central Brazil, *Anais da Academia Brasileira de Ciências* (submitted).

Fojtíková, L. (2014). http://www.irsm.cas.cz/materialy/oddeleni/6/fojtikova/Hronov.pdf (last accessed September 2014).

Fojtíková, L., V. Vavryčuk, A. Cipciar, and J. Madarás (2010). Focal mechanisms of micro-earthquakes in the Dobrá Voda seismoactive area in the Malé Karpaty Mts. (Little Carpathians), Slovakia, *Tectonophysics* **492,** 213–229.

Godano, M., T. Bardainne, M. Regnier, and A. Deschamps (2011). Moment-tensor determination by nonlinear inversion of amplitudes, *Bull. Seismol. Soc. Am.* **101,** 366–378, doi: 10.1785/0120090380.

Godano, M., E. Gaucher, T. Bardainne, M. Regnier, A. Deschamps, and M. Valette (2010). Assessment of focal mechanisms of microseismic events computed from two three-component receivers: Application to the Arkema-Vauvert field (France), *Geophys. Prospect.* **58,** 775–790, doi: 10.1111/j.1365-2478.2010.00906.x.

Hungarian Earthquake Bulletin. Kövesligethy Radó Seismological Observatory, MTA CSFK GGI, Budapest, Hungary 2014. HU ISSN: 1589-9756 (online), HU ISSN: 1589-8326 (printed).

Janský, J., V. Plicka, and J. Zahradník (2012). Re-evaluating possibilities of the source scanning algorithm, *Geophys. Res. Abstr.* **14,** EGU2012-4104, 2012, EGU General Assembly 2012.

Kagan, Y. Y. (1991). 3-D rotation of double-couple earthquake sources, *Geophys. J. Int.* **106,** 709–716, doi: 10.1111/j.1365-246X.1991.tb06343.x.

Křížová, D., J. Zahradník, and A. Kiratzi (2013). Resolvability of isotropic component in regional seismic moment tensor inversion, *Bull. Seismol. Soc. Am.* **103,** 2460–2473, doi: 10.1785/0120120097.

Li, J., H. Zhang, H. S. Kuleli, and M. N. Toksoz (2011). Focal mechanism determination using high-frequency waveform matching and its application to small magnitude induced earthquakes, *Geophys. J. Int.* **184,** 1261–1274, doi: 10.1111/j.1365-246X.2010.04903.x.

Nakamura, M. (2002). Determination of focal mechanism solution using initial motion polarity of P and S waves, *Phys. Earth Planet. In.* **130,** 17–29.

Novotný, O., and L. Urban (1988). Seismic models of the Bohemian Massif and some adjacent regions derived from deep seismic soundings and surface wave investigations: A review, in *Induced Seismicity and Associated Phenomena I*, D. Procházková (Editor), *Proc. of conference in Liblice*, 14–18 March, 1988.

Novotný, O., J. Zahradník, and G.-A. Tselentis (2001). Northwestern Turkey earthquakes and the crustal structure inferred from surface waves observed in western Greece, *Bull. Seismol. Soc. Am.* **91,** 875–879.

Pinar, A., K. Kuge, and Y. Honkura (2003). Moment tensor inversion of recent small to moderate sized earthquakes: implications for seismic hazard and active tectonics beneath the Sea of Marmara, *Geophys. J. Int.* **153,** 133–145, doi: 10.1046/j.1365-246X.2003.01897.x.

Serpetsidaki, A., N. K. Verma, G.-A. Tselentis, N. Martakis, K. Polychronopoulou, and P. Petrou (2013). Seismotectonics of lower Assam, northeast India, using the data of a dense microseismic network, *Bull. Seismol. Soc. Am.* **103,** 2875–2883.

Snoke, J. A. (2003). FOCMEC: FOcal MEChanism determinations, in *International Handbook of Earthquake and Engineering Seismology*, Chapter 85.12, W. H. K. Lee, H. Kanamori, P. C. Jennings, and C. Kisslinger (Editors), Academic Press, San Diego, California.

Sokos, E., and J. Zahradník (2008). ISOLA a Fortran code and a Matlab GUI to perform multiple-point source inversion of seismic data, *Comput. Geosci.* **34,** 967–977.

Sokos, E., and J. Zahradník (2013). Evaluating centroid-moment-tensor uncertainty in the new version of ISOLA software, *Seismol. Res. Lett.* **84,** 656–665.

Sokos, E., J. Zahradník, A. Kiratzi, J. Janský, F. Gallovič, O. Novotný, J. Kostelecký, A. Serpetsidaki, and G.-A. Tselentis (2012). The January 2010 Efpalio earthquake sequence in the western Corinth Gulf (Greece), *Tectonophysics* **530/531,** 299–309.

Vavryčuk, V. (2011). Tensile earthquakes: Theory, modeling, and inversion, *J. Geophys. Res.* **116,** no. B12320, doi: 10.1029/2011JB008770.

Villegas, R., S. Nacif, and S. Spagnotto (2014). Resolución y análisis de mecanismos focales de sismos corticales en cordillera entre 34.5° S y 36° S (abstract), special issue, *Earth Sci. Res. J.* **18,** 175–176.

Vuan, A., P. Klin, G. Laurenzano, and E. Priolo (2011). Far-source long-period displacement response spectra in the Po and Venetian plains (Italy) from 3D wavefield simulations, *Bull. Seismol. Soc. Am.* **103,** 1055–1072, doi: 10.1785/0120090371.

Wéber, Z. (2009). Estimating source time function and moment tensor from moment tensor rate functions by constrained L1 norm minimization, *Geophys. J. Int.* **178,** 889–900.

Zahradník, J., and S. Custódio (2012). Moment tensor resolvability: Application to southwest Iberia, *Bull. Seismol. Soc. Am.* **102,** 1235–1254, doi: 10.1785/0120110216.

Zahradník, J., and A. Plešinger (2005). Long-period pulses in broadband records of near earthquakes, *Bull. Seismol. Soc. Am.* **95,** 1928–1939, doi: 10.1785/0120040210.

Zahradník, J., and A. Plešinger (2010). Toward understanding subtle instrumentation effects associated with weak seismic events in the near field, *Bull. Seismol. Soc. Am.* **100,** 59–73, doi: 10.1785/0120090087.

Zahradník, J., and E. Sokos (2014). The M_w 7.1 Van, Eastern Turkey, earthquake 2011: Two-point source modelling by iterative deconvolution and non-negative least squares, *Geophys. J. Int.* **196,** 522–538, doi: 10.1093/gji/ggt386.

Lucia Fojtíková[1]
Institute of Rock Structure and Mechanics
Academy of Sciences of the Czech Republic
V Holešovičkách 94/41
182 09, Prague 8, Czech Republic
fojtikova@irsm.cas.cz

Jiří Zahradník
Charles University in Prague
Faculty of Mathematics and Physics
Department of Geophysics
V Holešovičkách 2
180 00 Prague 8, Czech Republic
jiri.zahradnik@mff.cuni.cz

[1] Also at Geophysical Institute, Slovak Academy of Sciences, Dúbravská cesta 9, 845 28 Bratislava, Slovak Republic.